Shape Change Through Programmable Stiffness

Michael McEvoy and Nikolaus Correll

University of Colorado at Boulder,
Department of Computer Science,
Boulder, CO 80309
{michael.mcevoy,nikolaus.correll}@colorado.edu
http://correll.cs.colorado.edu/

Abstract. We present a composite material with embedded sensing and actuation that can perform permanent shape changes by temporarily varying its stiffness and applying an external moment. Varying stiffness is a complementary approach to actuator-chain based approaches that can be accomplished using a large variety of means ranging from heat, electric field or vacuum. A polycaprolactone (PCL) bar provides stiffness at room temperature. Heating elements and thermistors are distributed along the bar so that local regions can be tuned to a specific temperature/stiffness. Applying an external moment using two tendon actuators then lets the material snap into a desired shape. We describe the composite structure, the principles behind shape change using variable stiffness control, and forward and inverse kinematics of the system. We present experimental results using a 5-element bar that can assume different global conformations using two simple actuators.

Keywords: Multi-functional Materials, Embedded Computation, Variable Stiffness

1 Introduction

Structural materials with the ability to change their shape have the potential to enable a new class of robotic devices ranging from assistive wearable technologies to morphable airplane wings [1,2] and furniture [3]. Providing the necessary actuation is a key challenge, in particular as individual actuators need to be strong enough to deform, and possibly support, the entire structure. We propose a novel approach to shape change based on programmable stiffness, which combines large numbers of variable stiffness elements [4] with a small number of actuators that extend over and are strong enough to deform an entire structure. Ideally, shape change and variable stiffness control, which includes actuation, sensing and local feedback control are integrated into the composite material itself. We dub this new class of materials "robotic materials" (RM) [4].

Our goal is to develop a RM that can change its shape and then lock it into a rigid configuration. When designing something that will change it's shape, the traditional approach is to use mechanical linkages and actuator chains. In

Fig. 1: Applications for a shape changing Robotic Material range from multi-functional furniture to shape-changing aerodynamic surfaces on boats, cars and aircraft.

contrast, we propose using smart materials that have the ability to change their stiffness.

We believe that multi-DOF shape change in a material can be achieved through a change in stiffness and the application of simple 1-DOF forces. Beam theory states that the curvature through a given section of a beam is only a function of the stiffness and the applied loads. We show that the curvature is not affected by the stiffness of neighboring regions, implying that distributed control of the stiffness in a beam could be used in conjunction with simple external loads to generate arbitrary vertical displacements in the beam. We also show how inverse kinematic solutions for the proposed shape-change material can be found using the inverse Jacobian method.

2 Related Work

Existing approaches to high-DOF shape change are largely dominated by series actuator chains or modular robots [5], which suffer from the trade off between individual motor torque with weight and the requirement to deform or lift the entire system. More recently, [6, 7] have begun investigating pneumatic actuator chains, whose structural properties are limited by the available air pressure and valve technology. The proposed approach combines pneumatic actuation with the ability to vary stiffness of a structural material, which has been extensively studied. For example [8,9] construct a variable stiffness material by exploiting the temperature-dependent variable shear modulus of polymers sandwiched between metal bars. While the stiffness of the materials in [8, 9] is dominated by the metal bars, [10] presents a variable stiffness material based on Field's metal with embedded Joule heating that can achieve stiffness changes of four orders of magnitude, albeit being limited to be either on or off. Other approaches to variable stiffness control rely on hydrogel [11], particle jamming [3, 12] (which

both require valves and pumps), magneto-rheological [13–15] (which requires strong electro magnets), or mechanical effects [16] (requiring motors). While these materials provide a wide range of variable stiffness mechanisms to explore, to the best of our knowledge, these variable stiffness systems have never been combined with actuation to create shape-changing materials.

3 Principle of Operation

In this paper we demonstrate a variable stiffness RM with the ability to change its shape. This section describes the fundamental mechanics of materials equations on which we have designed our RM, the core material we have chosen for the design, the method that we use to apply external loads to physically deform the RM and the process involved with changing the RM from one configuration to another.

3.1 Mechanics of Materials

We have chosen to demonstrate the shape changing abilities of variable stiffness RMs with a beam. The shape of a beam is governed by the moments M applied along it's length, the stiffness E of the beam along the length, and the cross-sectional inertia I of the beam along it's length as shown in Equation 1.

$$\kappa(x,t) = \frac{v''(x,t)}{(1+v'(x,t)^2)^{\frac{3}{2}}} = \frac{M(x,t)}{E(x,t)I(x)} \tag{1}$$

Typically stiffness and cross-sectional inertia are fixed at the time of manufacture as E(x) and I(x), respectively. With variable stiffness RMs, we can now change the stiffness along the beam's length on demand so have E(x,t), i.e. the stiffness is now controllable as a function of time. This new ability allows a single actuation moment to induce a wide range of motion in the actuator.

3.2 Core Material

With advances in materials science, there are many examples of materials that can change their properties with the application of an external stimulus. Some of these materials and the morphing systems designed around them are highlighted in [2].

For the core material of our RM we use the thermoplastic polycaprolactone (PCL). Thermoplastics are inexpensive, easily manufactured and formed, and allow us to change their stiffness over multiple orders of magnitude simply by heating and cooling. Using Joule heating and temperature control, we can take advantage of the stiffness changes that occur as their temperature rises. PCL has a glass transition temperature of -50 C and is in its rubber state at room temperature. PCL has a Young's Modulus of approximately 190 MPa at room temperature and drops to nearly 2MP when molten (60 C). Further material properties for PCL are described in [17].

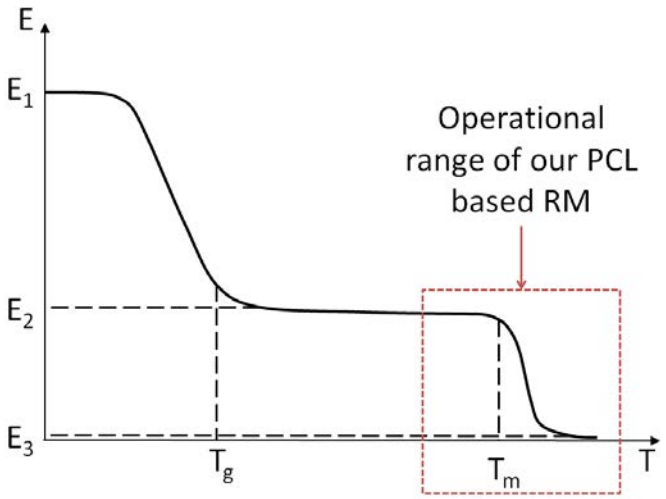

Fig. 2: For a typical thermoplastic, the Young's modulus drops when approaching the glass transition temperature and then drops again when approaching the melting temperature. It is this variation of Young's modulus with temperature change that we exploit in this particular RM.

3.3 Application of External Loads

To apply the external loads needed to change the beam's shape we use two mechanical actuators as in [18] that pull cables running along each side of the bar. This design choice allows us to leverage other results from the field of continuum robotics as described in Section 5.1. The cables are held in place by supports that are placed at increments along the length of the bar, leading to a number of discrete sections. Tension on the cables produces a constant moment M across each section and allows us to set either a positive or negative moments across all of the segments of the bar at once. This concept is shown in Figure 3.

Controlling the material properties in each of these sections allows for different curvatures to be produced in different sections of the bar while applying a single load to one of the cables. We note that shapes in which both positive and negative curvatures are present require a two-step process in which the bar first locks in all negative curvatures and then all positive curvatures (or the other way round).

Applying Equation 1 to a segmented RM with constant cross-section we obtain a piecewise function for the curvature of the beam. The continuity conditions state that the deflection curve is physically continuous and that the slopes for each segment of the beam must equal at the endpoints. Choosing to fix the base of the beam, we then have boundary conditions on the displacement and slope of the beam at it's base. The piecewise functions and the continuity and boundary

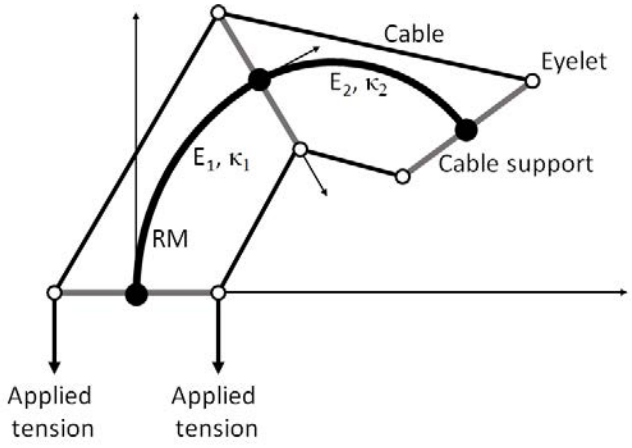

Fig. 3: A variable stiffness RM allows us to achieve different curvatures through different sections with only a single actuating force. The first section of the beam is set to a stiffness of E_1 while the second is set to E_2. With $E_1 > E_2$ we can get $\kappa_1 < \kappa_2$ by applying a single tension to the driving cable.

conditions are shown in Equation 2 where the subscript i denotes section number and A and B indicate a sections start and end points respectively.

$$\begin{aligned} \kappa_i(t) &= \frac{M(t)}{E_i(t)I} & \\ v_0(0,t) &= 0 & \text{Boundary Conditions} \\ v_0'(0,t) &= 0 & \\ v_i(B,t) &= v_{i+1}(A,t) & \text{Continuity Conditions} \\ v_i'(B,t) &= v_{i+1}'(A,t) & \end{aligned} \tag{2}$$

3.4 Shape Control

In order for a thermoplastic to be locked into a specific shape, it must be heated past its melting point and then allowed to cool while being held in that configuration. As noted in the previous section, the cables can be used to apply either a positive or negative moment across the beam, necessitating a two step process for shape changes involving both positive and negative curvatures. While this process poses some additional challenges (which we discuss in Section 7), we are able to demonstrate the possibilities of variable stiffness RMs and shape change using the following process (Figure 4).

We start with an undeformed beam without any load applied and program a stiffness profile to it (Fiqure 4a- 4b). Next a constant moment is applied along the length of the beam to deform its shape (Figure 4c). The cable is held at a constant

displacement while the PCL is heated to melting and then cooled, locking the shape of the deformed beam (Figures 4d- 4e). The process is repeated to produce curvatures in the opposite direction (Figure 4f), producing an arbitrary shape change in the beam.

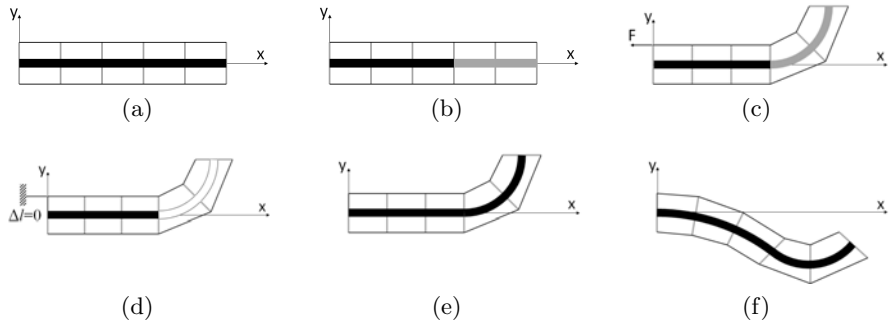

Fig. 4: A change in shape starts with an undeformed beam without any load applied (a). The segments that will have positive curvature are set to the appropriate stiffness, this change is noted by the light gray sections (b). Once the segment stiffnesses have been programmed, a load is applied to the cable, causing the segments to deform (c). The cable is then held at a constant displacement while the deformed sections are heated to melting, indicated by white (d). The segments return to their original stiffnesses and the cable tension is released, leaving the beam in the deformed state (e). This process is repeated for those segments with negative curvature and an arbitrary pose is achieved (f).

4 Fabrication

The core functionality of this RM is enabled by embedding sensing and actuation directly into the material, in this case, a thermistor and a nichrome heating element.

First, we form the PCL bar by melting pellets of PCL and pressing them into an acrylic mold along with a nylon mesh. A nylon mesh is embedded into the PCL to help maintain the cross-section when sections are heated very close to their melting temperature. The finished bar is 6.35 mm thick by 25.4 mm wide and is 311.15 mm long. Five 50.8 mm sections are marked off with a 31.75 mm section at the base and 25.4 mm section at the end for clamping and cable mounting purposes.

Next thermistors are embedded into the center of each section to monitor the temperature. Then each section is wrapped with a length nichrome wire which is secured to the beam with Kapton tape. The nichrome wire is wrapped around the bar with a 5.08 mm spacing, resulting in a resistance of $48 \pm 1\Omega$ per section.

Finally the entire bar is encapsulated in a thin layer of silicone to insulate the heating elements from the environment and help maintain the cross-sectional shape for sections heated very near the melting point. A schematic of the design is shown in Figure 5 and can be seen in the experimental setup in Figure 7.

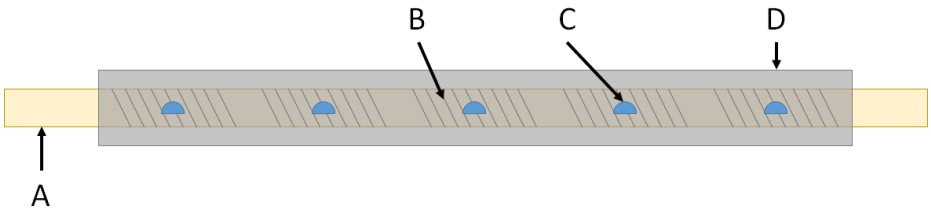

Fig. 5: The demonstrated RM consists of a PCL bar (A), nichrome heating elements to heat the individual sections (B), embedded thermistors to monitor and control the temperature of each section (C), and an encasing of silicon (D) for insulation and to help maintain the cross-section when sections are heated close to the melting temperature.

Determination of the temperature propagation through the sections as well as sectional heat-up and cool-down cycles using a similar design are described in [4].

Our RM is made completely from commercial-off-the-shelf products. We use PCL sold by SparkFun Electronics under the trade name PolyMorph (TOL-10951), 36 gage Nichrome 60 wire from Jacobs Online, thermistors from Digi-Key (490-4664-ND), and Ecoflex 00-30 silicon from Smooth-on.

5 Control

Our choice to use a cable driven system to apply the forces necessary for shape change allow us to utilize forward and inverse kinematics results from the continuum robotics field [7, 19]. A short overview of these results and how they are applied to our RM is given in this section.

5.1 Forward Kinematics

We propose to model the variable stiffness RM using Piecewise Constant Curvature (PCC) models from continuum robotics. PCC assumes that the curvature in a section is constant so that the forward kinematics are treated as consecutive transformations as shown in Figure 6a where the transformation from the coordinate system of section $i+1$ to section i is governed by Equation 3, where $x_0 = y_0 = \theta_0 = 0$.

$$\begin{bmatrix} x_i \\ y_i \\ \theta_i \end{bmatrix} = \begin{bmatrix} cos(\theta_{i-1}) & sin(\theta_{i-1}) & 0 \\ -sin(\theta_{i-1}) & cos(\theta_{i-1}) & 0 \\ 0 & 0 & 1 \end{bmatrix} \begin{bmatrix} \kappa_i^{-1}\left(1 - cos\left(\kappa_i s_i\right)\right) \\ \kappa_i^{-1} sin\left(\kappa_i s_i\right) \\ 0 \end{bmatrix} + \begin{bmatrix} x_{i-1} \\ y_{i-1} \\ \theta_{i-1} \end{bmatrix} \tag{3}$$

The local coordinates along a segment are given by Equation 4 and shown in Figure 6b.

$$\begin{aligned} x &= \kappa_i^{-1}\left(1 - cos\left(\kappa s\right)\right) \\ y &= \kappa_i^{-1} sin\left(\kappa s\right) \\ \theta &= \kappa s \end{aligned} \tag{4}$$

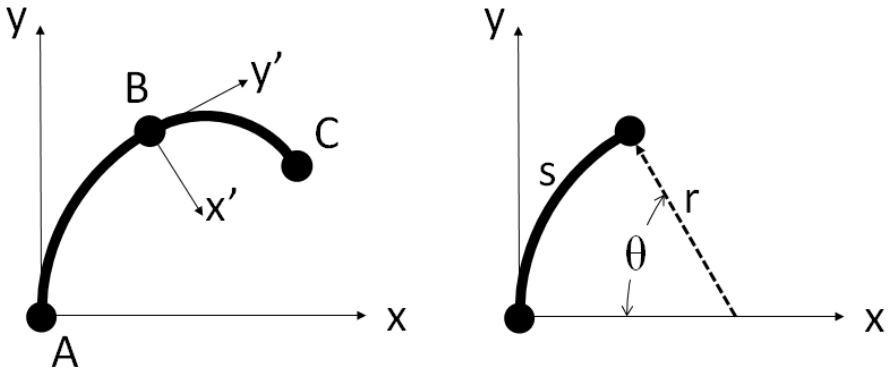

(a) (b)

Fig. 6: Assuming that the curvature in each section of the RM is constant, the forward kinematics is a series of transformations for each section. Knowing the curvatures for each section fully defines the pose of the RM.

5.2 Inverse Kinematics

As it is infeasible to find analytical solutions for the inverse of (3) for large numbers of segments, we chose an inverse Jacobian method as described in [7,19] for this class of robot. This approach also allows us to impose limits on the sectional curvatures so that the proposed pose changes are always reachable. Let Δx, Δy and $\Delta\theta$ be small changes from the current pose of the beam in the direction of a desired pose $(x, y, \theta)'$. We can then write

$$(\Delta x, \Delta y, \Delta\theta)' \approx J(\Delta\kappa_1, ..., \Delta\kappa_n)' \tag{5}$$

where J is a Jacobian matrix with dimension [3xn] containing the partial derivatives $\frac{\partial x}{\partial \kappa_i}$, $\frac{\partial y}{\partial \kappa_i}$, and $\frac{\partial \theta}{\partial \kappa_i}$ with $i = [1..n]$ and n the number of segments. These partial derivatives can be calculated analytically from (3) .

Appropriate values for the curvature of each segment can now be calculated from (5) by calculating the pseudoinverse $J^+ = J(J^T J)^{-1}$. As each individual segment is a single beam that adheres to (1), we can calculate the required $M/E(i)$ ratio, and therefore the temperature we need to set a bar, by $M/E(i) = I\kappa(i)$.

6 Experiments

In this section we detail the experimental setup, how we determined section curvatures as a function of temperature, and step through an example using these values to achieve a desired pose.

6.1 Experimental Setup

The experiments are conducted with the five section PCL bar described in Section 4. The bar is mounted to a table and deflections of the beam are limited to the plane of the table. Each section is monitored and controlled by a central computer. The tension applied to either of the cables is limited to 9.8 N. This restriction helps to emphasize the range of motion possible using only a single actuation force, but need not be limited in other applications. An overview of the experimental setup is shown if Figure 7.

During each test, the temperature histories of each section are recorded along with the fiducial positions of the section endpoints.

6.2 Determining $\kappa(T)$

In the first set of experiments we capture the range of motion of our device and also characterize the relationship between curvature and temperature. For this series of tests, a tension is applied to either the left or right cable while the beam is held at a uniform temperature. Displacements are recorded at various temperatures between room temperature and 50 C with each test being repeated five times for a total of 80 trials. The range of motion of our RM is shown in Figure 8, where the five trials for each temperature have been averaged. After collecting the data from each of the tests the displacements of each of the section ends was averaged for each temperature and curvatures through each section were found using a least-squares method and the PCC assumption. Figure 9 shows the results of this process, with the expected result that the curvature increases dramatically as the temperature reaches the melting point. Of note is that not centering the mesh in the PCL resulted in asymmetric positive and negative curvatures.

The error in curvature tends to increase with temperature. This is somewhat expected since we are in a steeper region of the E vs. T region (Figure 2).

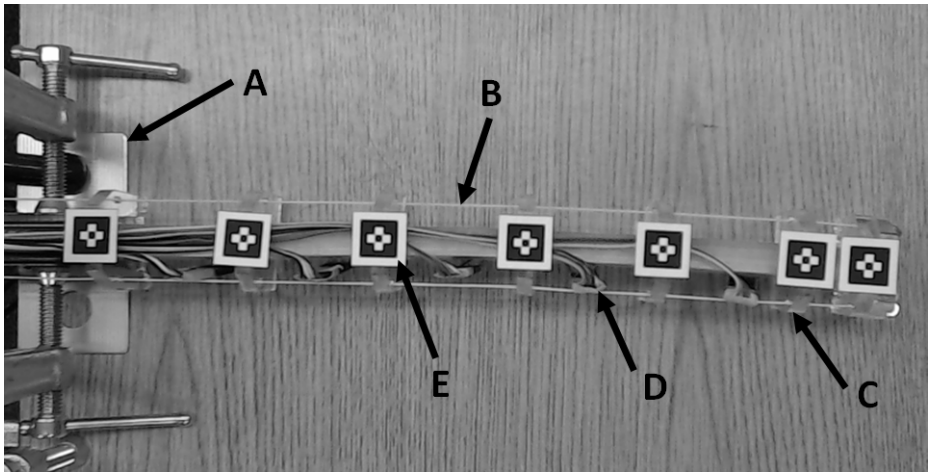

Fig. 7: For the experiments, the PCL bar is clamped to a table (A). Cables (B) are routed through sliders (C) and apply a constant moment along the length of the bar when tension is applied to the cables. Each section's thermistor and nichrome heater are connected to the control computer (D), and the displacement of each section is monitored by tracking a fiducial (E).

6.3 Inverse kinematics

To verify that our RM can achieve a desired pose, we take a reachable point from Figure 8and use the IK solver to find a possible set of sectional curvatures to be applied to each section. We then use the two step process outlined in Section 3.4 to achieve the desired pose. Figure 10 shows the results of this open-loop control including intermediate shapes and the resulting error.

7 Experimental Insights

Our variable stiffness RM is able to change shapes using a constant actuation force and programmable stiffness of its sections. This first-of-its-kind programmable material demonstrates the possibilities of RMs with respect to shape change, but also offers new challenges in design and control.

When determining the curvature vs. temperature profiles we assumed that all sections would have the same curvature, however inconsistencies in manufacturing of the bar and of the heating elements need to be addressed. We found that slight variations in the heating elements caused nonuniform heating of the PCL in each section. In addition, the manufacturing process of the PCL bar left slight variations in the thickness of the bar, but at the time of fabrication, bars of PCL were not commercially available. Addressing these issues will serve to decrease the error found in the curvature vs. temperature (Figure 9).

Setting of the thermoplastic into the desired shape (Figure 4 c-e) also poses some control problems not addressed by our RM. Figure 12b shows a two segment

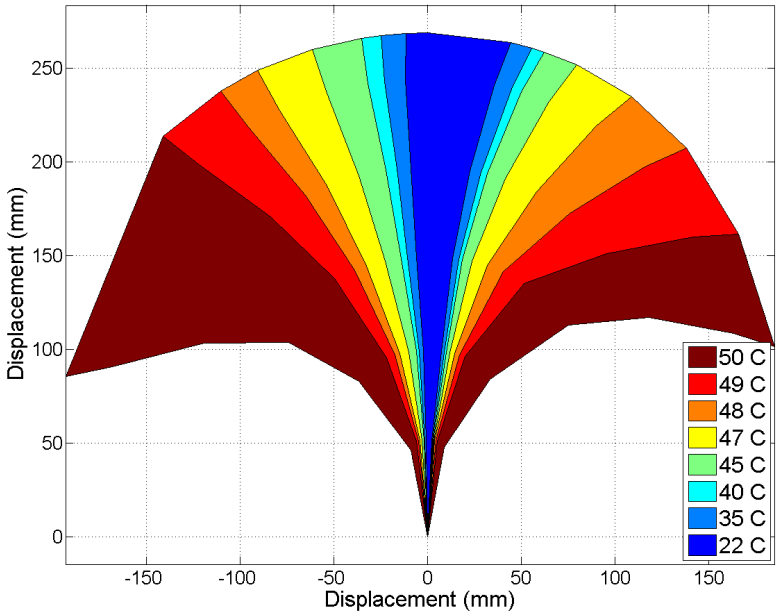

Fig. 8: The range of motion of the variable stiffness RM. When all of the heating elements in the beam are off, the stiffness is at a maximum and the displacement in the beam is limited. Activating all of the heating elements the stiffness of the beam is at a minimum and a much larger range of motion is achieved using the same actuation force.

RM where end section has been set to the desired stiffness, E_2 and needs to be locked into this shape. When locking the section into place, the temperature is raised to melting. The stiffness in this section is lowered to E_3, which is accompanied by an increase in curvature. Since the cable's length is held constant during this process, the fore section relaxes a proportional amount as seen in Figure 12b. To avoid this problem, additional control needs to be implemented to adjust the temperature of the other sections.

Due to the large variation in material properties, the accuracy of open loop control is severely limited. This limitation could be overcome by implementing a closed loop control scheme that does not only rely on thermistors, as in this paper, but also on embedded curvature sensors. We note that such a controller can also be implemented in a fully distributed way as the overall shape is only dependent on local curvatures.

In order for the proposed approach to work repeatably, care must be taken to limit force and stiffness combinations so that the material does not yield. Too great of a force would mean that the material would yield and plastically deform

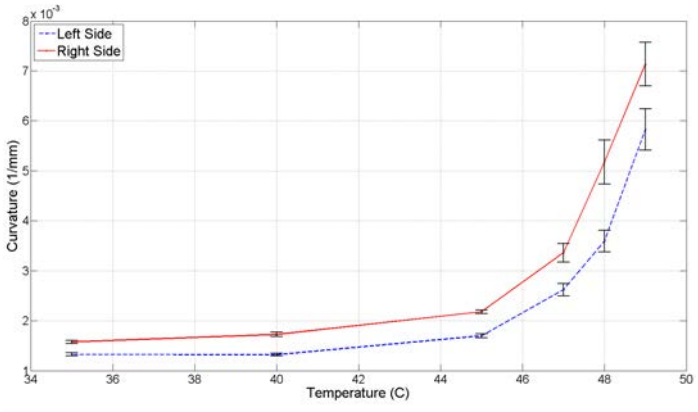

Fig. 9: The curvature increases dramatically as the temperature approaches melting.

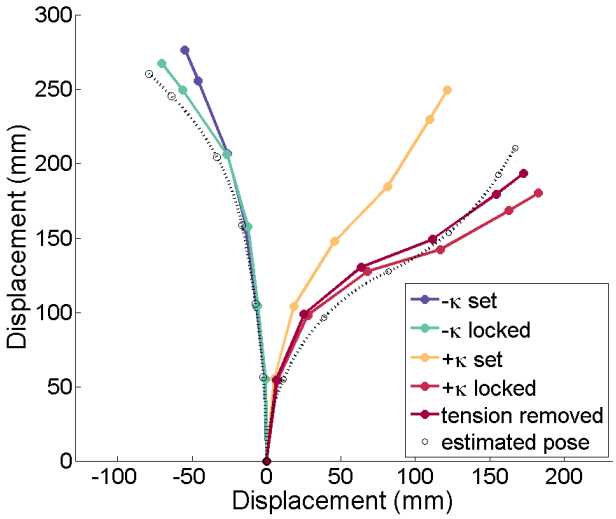

Fig. 10: To reach a desired pose, we first set the negative curvatures found by the IK solution and lock them in before programming the positive curvature sections. The dashed lines are what we expect from the forward kinematics. The change in pose from setting the $+\kappa$ sections and locking them is discussed in Section 7

.

and the beam would no longer be operating in the region where Hooke's law applies.

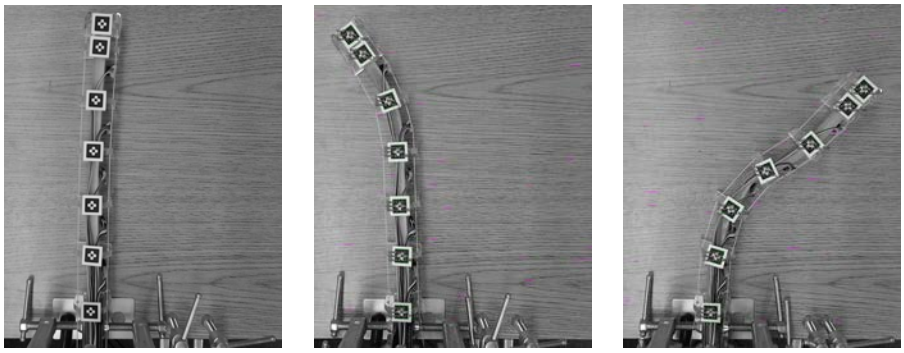

(a) (b) (c)

Fig. 11: Snapshots from the experimental trial shown in Figure 10. (a) shows the initial position of the RM, (b) shows the RM after setting the negative curvatures and (c) shows the pose after setting the positive curvatures.

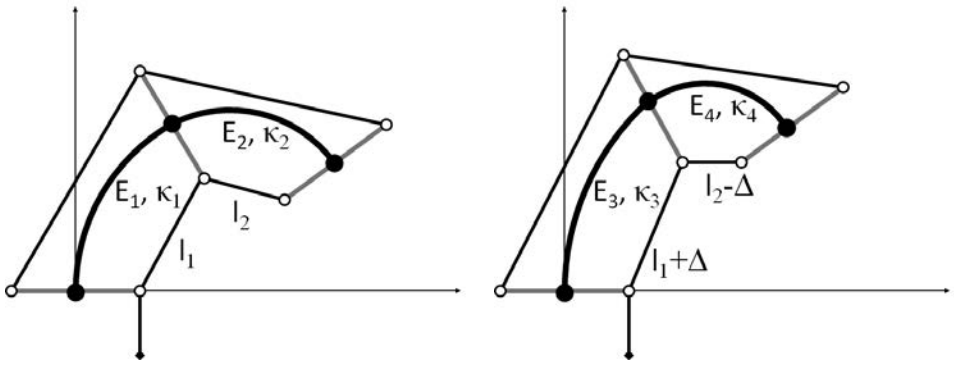

(a) (b)

Fig. 12: (a) shows a RM where κ_2 has been set and needs to be locked. When locking in the curvature, the thermoplastic must be raised to melting, which corresponds in a drop in stiffness $E_2 > E_4$ (b). If the temperature of section one is not adjusted, the change in stiffness will cause a change in the curvatures from $\{\kappa_1, \kappa_2\}$ to $\{\kappa_3, \kappa_4\}$ as the first section relaxes and the second section increases in curvature.

A limitation of the proposed shape-change using variable stiffness approach is that the necessary motions to achieve even subtle shape changes can be quite large. This is nicely illustrated in Figure 10. In order to reach the desired final position to the right, the material first needs to bend to the left. This can only be overcome by adding additional actuators throughout the RM, trading the limitations of this approach with that of conventional multi-link robotic systems.

We chose tendon-based actuators in this paper as they provide a good force-to-weight ratio since the tendons can be installed at a distance from the material. However, any actuator that can provide a constant moment across the length of the beam is suitable. For example, we have also considered pneumatic actuators as in [6]. While these actuators can provide large moments, they add considerably to the thickness of the material, resulting in an increased cross-sectional inertia and an overall smaller range of motion.

8 Conclusion

We demonstrate experimentally that shape change can be obtained by locally varying the stiffness of a material and applying a single external moment. The experiments show that the proposed shape-changing material can indeed reach a wide range of possible shapes that are only limited by the available external moments and the properties of the material itself.

Relying on melting via joule heating allows to reach good structural stability, but is power intense, slow, and dependent on the environment temperature. In the future, we wish to investigate other approaches for stiffness control, including electro-rheological fluids and pneumatic jamming. We would also like to investigate other actuators that provide good force to weight ratios, such as twisted wires, pulleys, and McKibbon-style actuators.

There is a trade-off between range of motion and structural stiffness. Structures that require a large range of motion will need to be very thin and thus will only be able to support small loads. Structures that require only a limited range of motion could potentially support larger actuators and support heavier loads.

Although the properties of variable stiffness robotic materials are compelling, we observe that their control is much more challenging then conventional, stiff actuator chains. In order to make such RMs accurate and precise, we will not only need to investigate embedded sensing and feedback control to overcome differences in polymer, actuators, and sensors, but also investigate novel manufacturing techniques to make such systems. In return, such robotic materials might not only be able to accurately change their shape, but also to respond to disturbances and damages in unprecedented ways.

Acknowledgments. This work has been supported by the Airforce Office of Scientific Research under grant number FA9550-12-1-0145, the National Science Foundation under grants number #1150223 and #1153158, and a Beverly Sear's Graduate Student Research Grant. We are grateful for this support.

References

1. Vasista, S., Tong, L., Wong, K.: Realization of morphing wings: A multidisciplinary challenge. Journal of Aircraft **49**(1) (2012) 11–28
2. Weisshaar, T.A.: Morphing aircraft systems: Historical perspectives and future challenges. Journal of Aircraft **50**(2) (2013) 1–17

3. Ou, J., Yao, L., Tauber, D., Steimle, J., Niiyama, R., Ishii, H.: jamSheets: thin interfaces with tunable stiffness enabled by layer jamming. In: Proceedings of the 8th International Conference on Tangible, Embedded and Embodied Interaction, ACM (2014) 65–72
4. McEvoy, M.A., Correll, N.: Thermoplastic variable stiffness composites with embedded, networked sensing, actuation, and control. Journal of Composite Materials (2014)
5. Yim, M., Zhang, Y., Duff, D.: Modular robots. Spectrum, IEEE **39**(2) (2002) 30–34
6. Correll, N., Onal, C.D., Liang, H., Schoenfeld, E., Rus, D.: Soft autonomous materials—using active elasticity and embedded distributed computation. In: 12th International Symposium on Experimental Robotics, Springer Tracts in Advanced Robotics Vol 79. (2014) 227–240
7. Marchese, A.D., Konrad, K., Onal, C.D., Rus, D.: Design, curvature control, and autonomous positioning of a soft and highly compliant 2D robotic manipulator. In: 2014 IEEE Int. Conf. Robotics and Automation, IEEE (2014)
8. Gandhi, F., Kang, S.G.: Beams with controllable flexural stiffness. Smart Materials and Structures **16**(4) (2007) 1179–1184
9. Murray, G., Gandhi, F.: Multi-layered controllable stiffness beams for morphing: energy, actuation force, and material strain considerations. Smart Materials and Structures **19**(4) (2010) 11
10. Shan, W., Lu, T., Majidi, C.: Soft-matter composites with electrically tunable elastic rigidity. Smart Materials and Structures **22**(8) (2013) 085005
11. Shanmuganathan, K., Capadona, J.R., Rowan, S.J., Weder, C.: Biomimetic mechanically adaptive nanocomposites. Progress in Polymer Science **35**(1) (2010) 212–222
12. Brown, E., Rodenberg, N., Amend, J., Mozeika, A., Steltz, E., Zakin, M.R., Lipson, H., Jaeger, H.M.: Universal robotic gripper based on the jamming of granular material. Proceedings of the National Academy of Sciences **107**(44) (2010) 18809–18814
13. Majidi, C., Wood, R.J.: Tunable elastic stiffness with microconfined magnetorheological domains at low magnetic field. Applied Physics Letters **97**(16) (2010) 164104–164104
14. Chen, J., Liao, W.: Design, testing and control of a magnetorheological actuator for assistive knee braces. Smart Materials and Structures **19**(3) (2010) 035029
15. Varga, Z., Filipcsei, G., Zrínyi, M.: Magnetic field sensitive functional elastomers with tuneable elastic modulus. Polymer **47**(1) (2006) 227–233
16. Pratt, G.A., Williamson, M.M.: Series elastic actuators. In: Intelligent Robots and Systems 95.'Human Robot Interaction and Cooperative Robots', Proceedings. 1995 IEEE/RSJ International Conference on. Volume 1., IEEE (1995) 399–406
17. Averous, L., Moro, L., Dole, P., Fringant, C.: Properties of thermoplastic blends: starch–polycaprolactone. Polymer **41**(11) (2000) 4157–4167
18. Li, C., Rahn, C.D.: Design of continuous backbone, cable-driven robots. Journal of Mechanical Design **124**(2) (2002) 265–271
19. Webster, R.J., Jones, B.A.: Design and kinematic modeling of constant curvature continuum robots: A review. The International Journal of Robotics Research **29**(13) (2010) 1661–1683